Supporting Information

Heterogeneous reservoir computing in second-order Ta_2O_5/HfO_2 memristors

Nestor Ghenzi [a,b], Tae Won Park[a], Seung Soo Kim[a], Hae Jin Kim[c], Yoon Ho Jang[a], Kyung Seok Woo*[a], and Cheol Seong Hwang*[a]

[a] *Department of Materials Science and Engineering and Inter-University Semiconductor Research Center, Seoul National University Gwanak-ro 1, Gwanak-gu, Seoul 08826, Republic of Korea*
[b] *Universidad de Avellaneda UNDAV.and Consejo Nacional de Investigaciones Científicas y Técnicas (CONICET), Argentina*
[c] *Department of Materials Science and Engineering, Myongji University, Yongin 17058, Korea*

corresponding author: kevinwoo@snu.ac.kr, cheolsh@snu.ac.kr

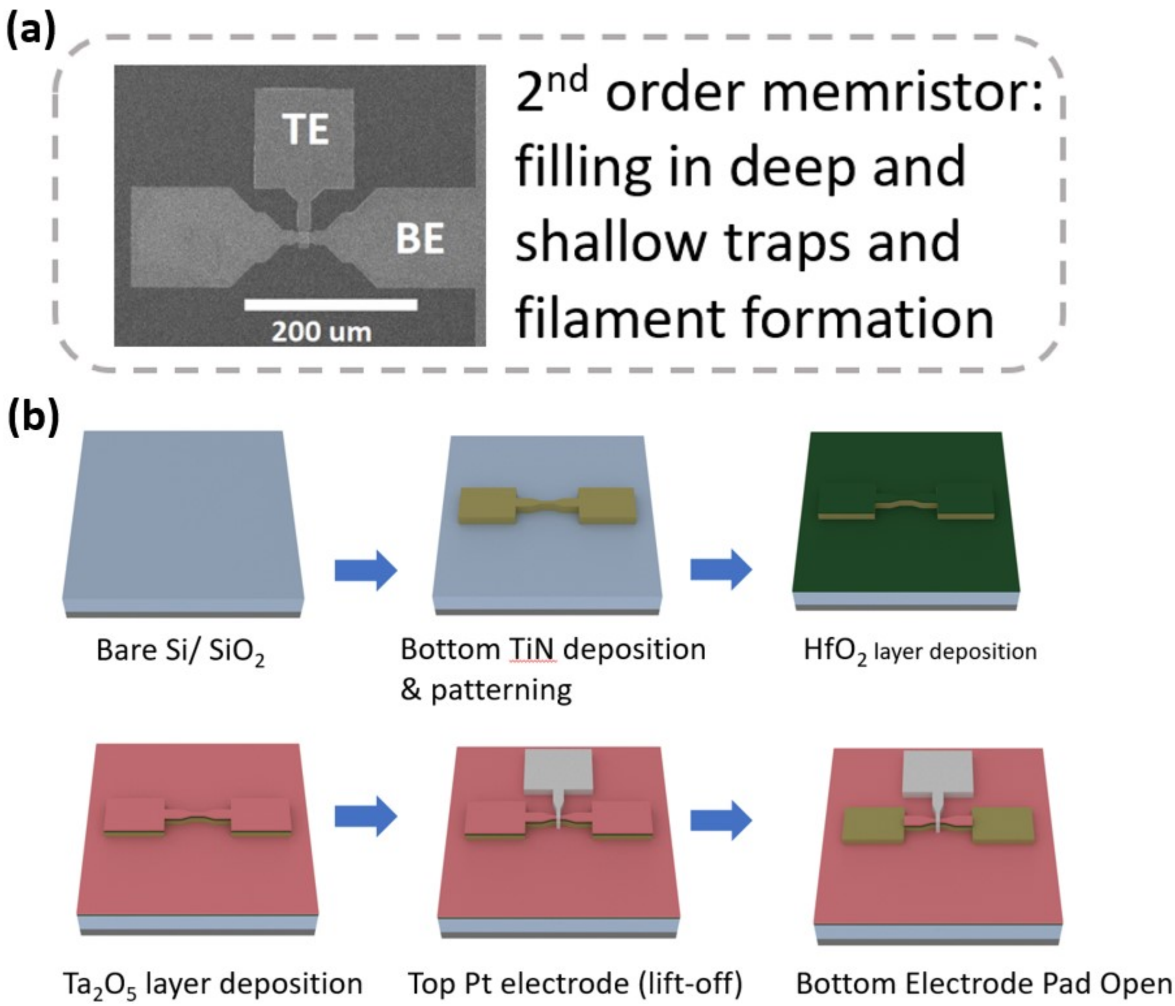

Fig. S1. ***(a) SEM image of a fabricated device with the flow process shown in (b). (b)*** **Process Flow of Pt/Ta_2O_5/HfO_2/TiN crosspoint device.**

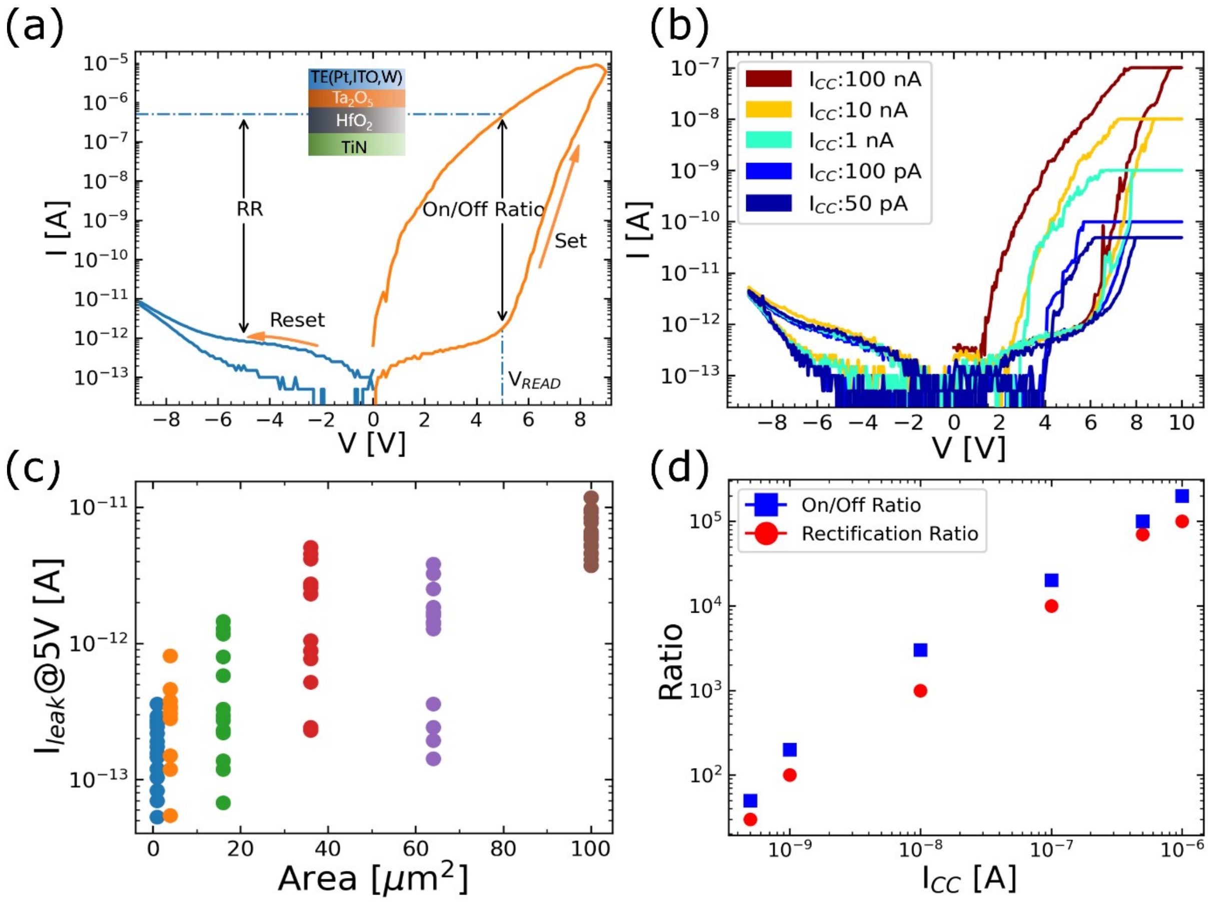

Fig. S2: **(a) DC I-V response of Pt/Ta_2O_5/HfO_2/TiN devices defining the ON/OFF ratio and the Rectification ratio. (b) Compliance current dependence on the self-rectifying mode. (c) The leakage current of the device in the HR state indicates uniform conduction in agreement with the charge-trapping mechanism. (d) The ON/OFF ratio and rectification ratio depend on the current compliance.**

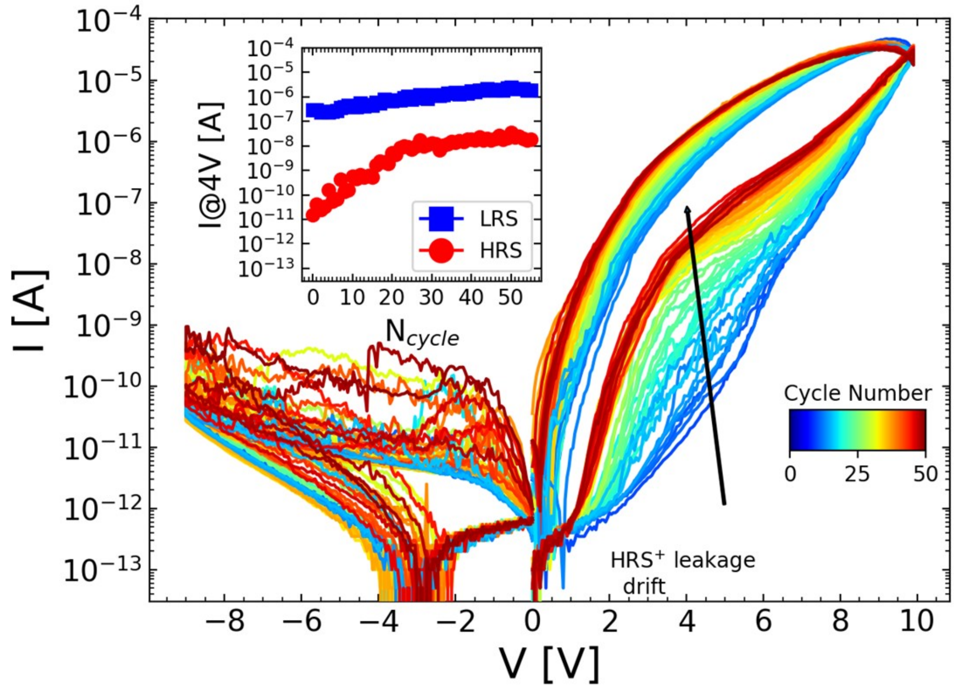

Fig S3. Leaky Ta_2O_5: 50-cycle DC measurement without current compliance.

To increase the knowledge about the leaky Ta_2O_5 layer, 50 cycles of I-V response with no external current compliance were measured, as shown in Fig. S3. After the first cycles, the current in negative polarities increases and becomes a noisy signal, in conjunction with a monotonous increase of the leakage current in the HRS in positive voltage polarity. The evolution of the current measured at 4 V is shown in the inset of Fig. S3. A high increase in the current value of the HRS can be seen for the first 20 cycles. This increase in the HRS current degrades the on/off ratio from ~ 4 to ~ 2 orders of magnitude.

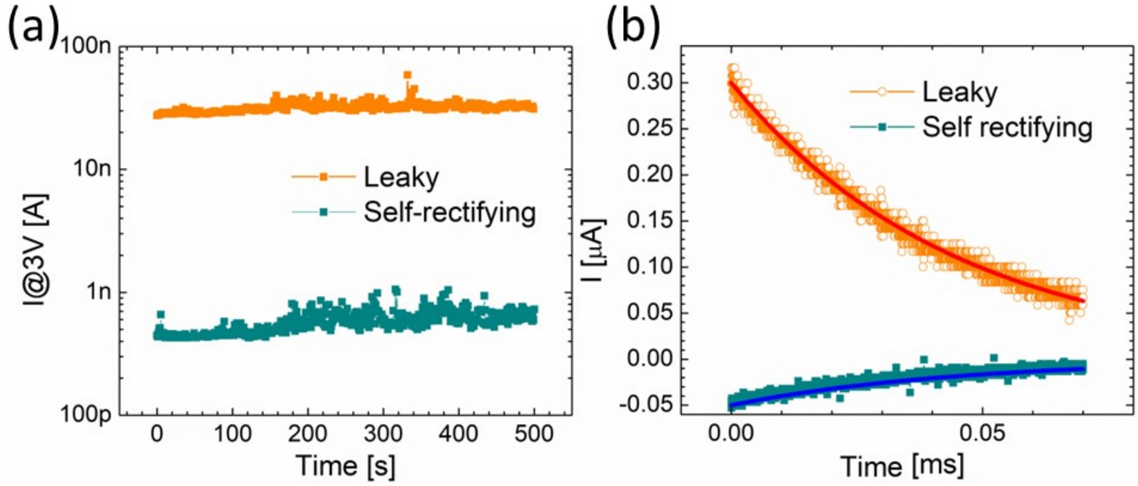

Figure S4. (a) Long retention characteristics of the low resistance state in the self-rectifying and leaky modes. Both modes present a stable conduction state. (b) A decay time of 50 μs in the current value for both modes is observed after a 12V pulse with 10 μs length is applied. Solid red and blue lines are the best-fitting results for the Leaky and self-rectifying modes, respectively.

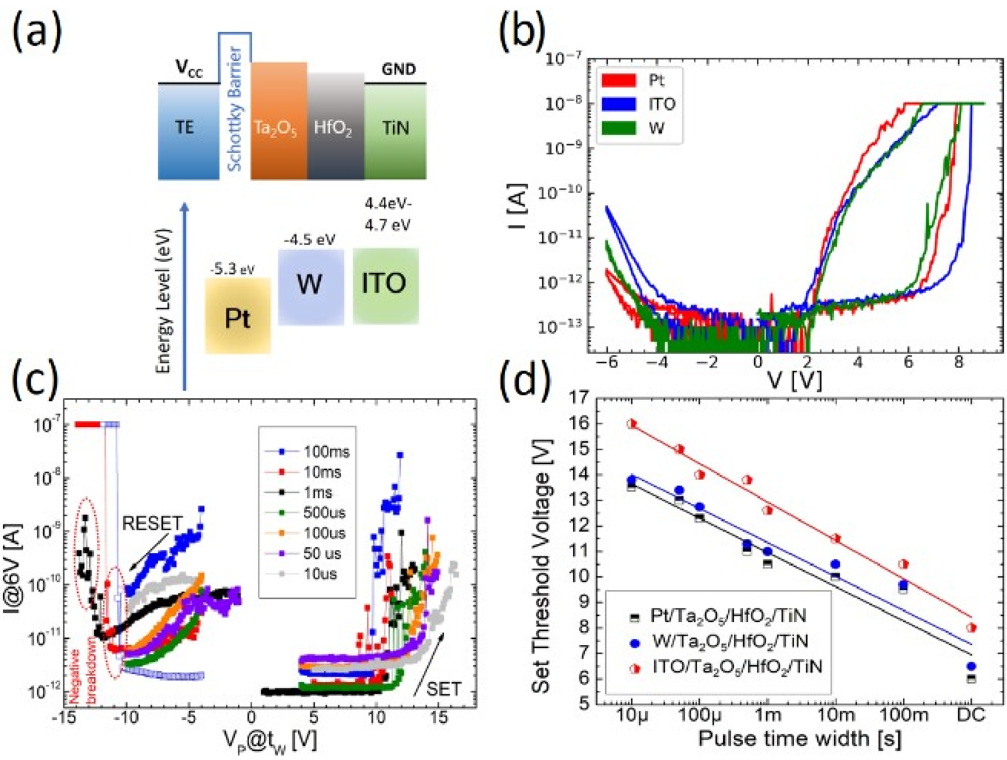

Fig. S5: **Electrode dependence: (a) Device structure with the bilayer Ta_2O_5/HfO_2 bilayer like the dielectric material. The TiN bottom electrode provides an ohmic contact with the HfO_2. The top electrode materials are Pt, W, and ITO. A Schottky barrier is formed between the TE material and the Ta_2O_5 layer. (b) I-V response with I_{CC} = 10 nA for the 3 top electrodes with HfO_2 undoped. The leakage current in the inverse direction and the SET voltage strongly depend on the types of electrodes, while the LRS current is invariant to the change of TE. (c) Voltage dependence of I_{READ} @6V at several pulse width voltage pulses. (d) Set threshold voltage dependence with the pulse time width.**

The SET threshold voltages were examined for different time widths for the samples with the 3 electrode materials (Pt, W, and (In, Sn)O (ITO), Fig. S4(a-b)). The measurement protocol consists of pulses of increasing amplitude until the conductance change is noticeable. The performance of devices was affected by the length of the pulse time, so it was necessary to explore the dynamic response to pulse widths from 10 µs to 100 ms and static DC I-V sweeps. Fig. S4(c) shows the measurements of the dynamic response to short pulses measured with V_{READ} = 6V after applying the pulses. This protocol was applied for the SET and RESET processes, but the RESET process did not clearly define an onset. Additionally, the negative threshold voltage to initiate the ion-based resistive switching overlaps with the RESET threshold, interfering with the threshold measurement. In the SET process, the onset was determined by extrapolating the increasing conductance value with a linear fit to the baseline of the initial conductance value. Fig. S4(d) plots the extracted onset value as a pair, the set threshold voltage, and pulse time width. The trend is almost exponential for all the explored devices, with similar behavior between different devices.

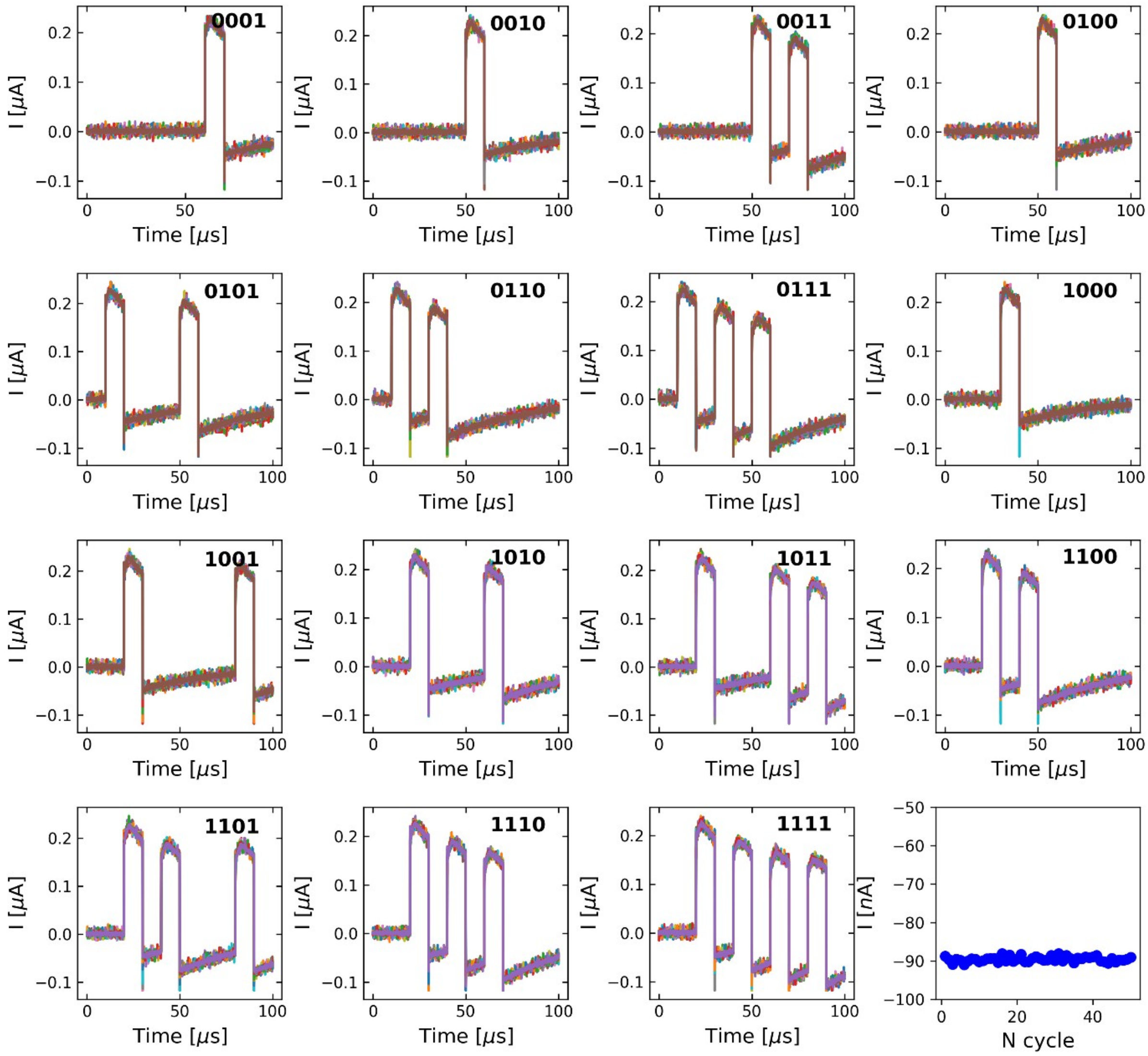

Fig S6. Response to 4-bit patterns in the self-rectifying mode. (bottom right) Evolution of current value for pattern 1111, where a random response is observed.

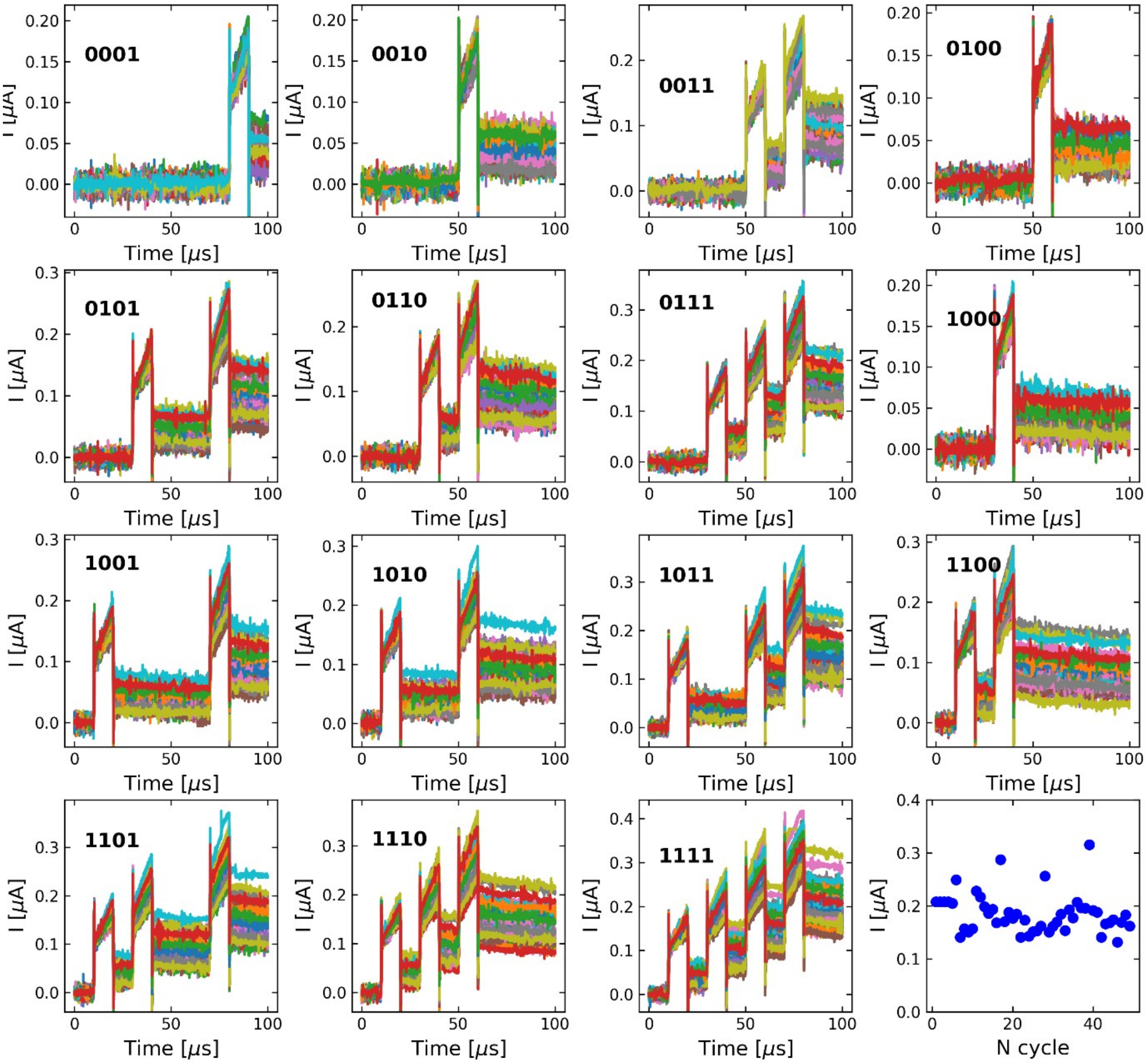

Fig S7. Response to 4-bit patterns in the Leaky mode. (bottom right) Evolution of current value for pattern 1111, where a random response is observed.

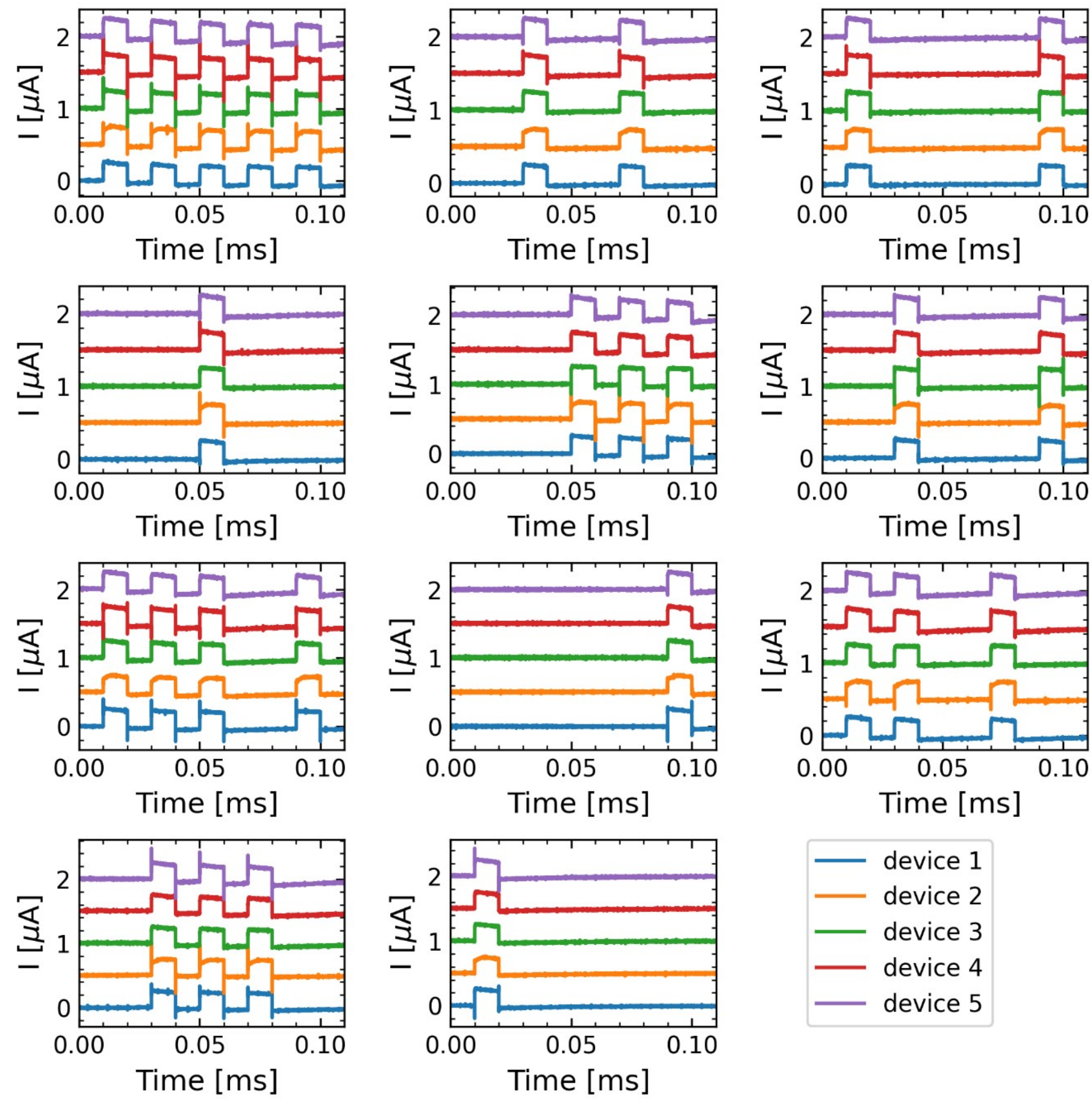

Figure S8. Experimental response to selected 5-bit patterns for 5 different PTHT memristor devices in the self-rectifying mode. The signals have been shifted by 500 nA to allow better comparison of the signals. These pulses were 12 V amplitude and 10 ms of time width, which did not change the device's non-volatile resistance, as shown in Figure S4. These figures show relevant patterns to determine the device-to-device variability of the devices: '11111', '01010', '10001', '00100', '00111', '01001', '11101', '00001', '11010', '01110' and '10000'.

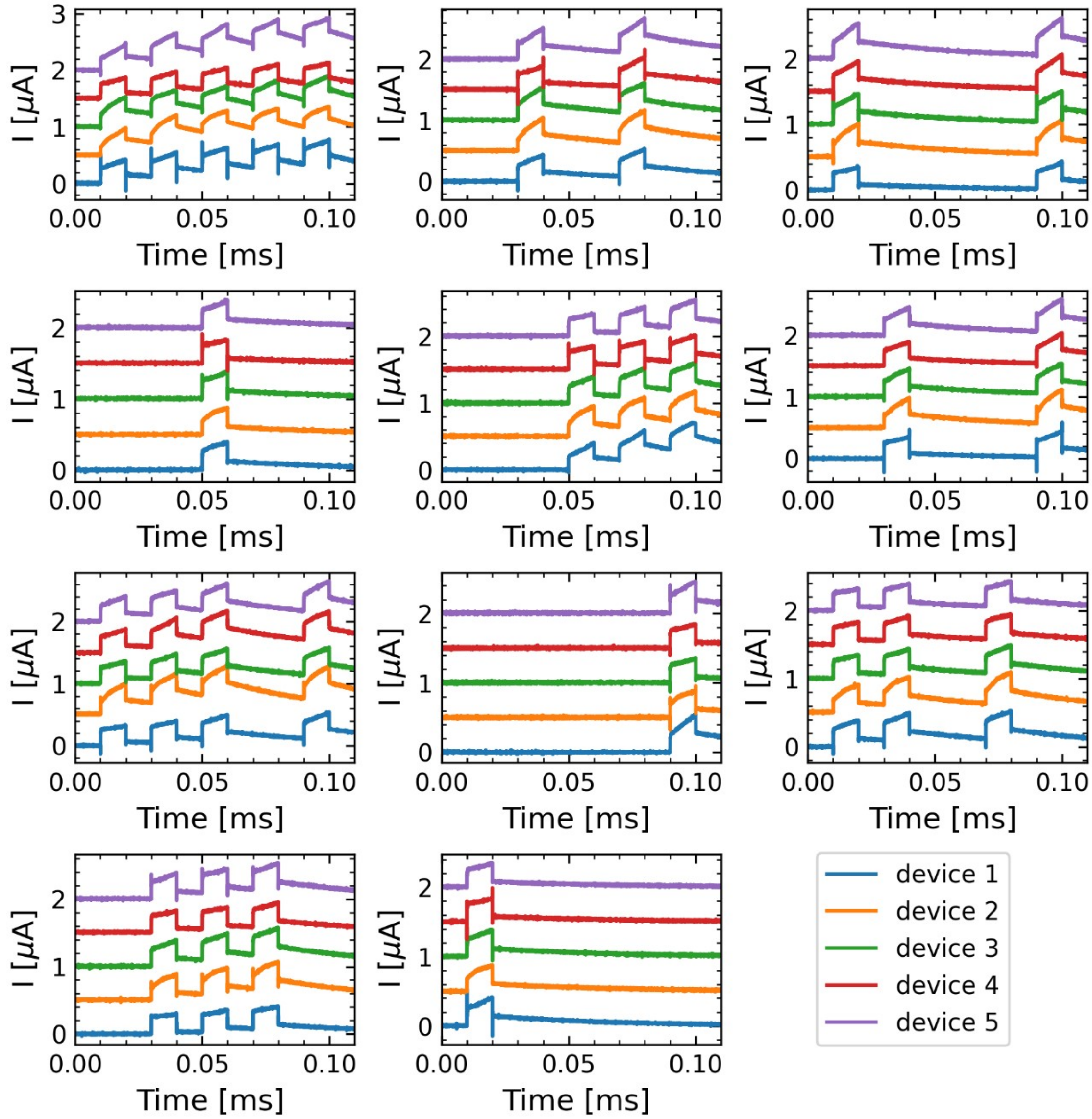

Figure S9. Experimental response in the leaky mode to selected 5-bit patterns to show device-to-device variability. Each signal has been shifted by 500 nA to allow better comparison of the signals. A similar increase in the current during consecutive pulses is observed in the different devices.